Journal of Alloys and Compounds 509 (2011) 3682–3685

Contents lists available at ScienceDirect

Journal of Alloys and Compounds

journal homepage: www.elsevier.com/locate/jallcom

Porous $Li_4Ti_5O_{12}$ anode material synthesized by one-step solid state method for electrochemical properties enhancement

Chih-Yuan Lin, Jenq-Gong Duh*

Department of Materials Science and Engineering, National Tsing-Hua University, Hsinchu, Taiwan

ARTICLE INFO

Article history:
Received 7 October 2010
Received in revised form
21 December 2010
Accepted 21 December 2010
Available online 28 December 2010

Keywords:
Lithium ion battery
Anode material
Porous $Li_4Ti_5O_{12}$

ABSTRACT

A porous $Li_4Ti_5O_{12}$ anode material was successfully synthesized from mixture of LiCl and $TiCl_4$ with 70 wt% oxalic acid by a modified one-step solid state method. The anode material $Li_4Ti_5O_{12}$ exhibited a cubic spinel structure and only one voltage plateau occurred around 1.5 V. The initial capacity of porous $Li_4Ti_5O_{12}$ was 167 and 133 mAh g^{-1} at 0.5 and 1*C* charge/discharge rate, respectively, and the capacity retention maintained above 98% after 200 cycles. The porous $Li_4Ti_5O_{12}$ structure showed promising rate performance with a capacity of 70 mAh g^{-1} at charge/discharge 10*C* rate after 200 cycles. It was demonstrated that the porous structure could withstand 50*C* charge/discharge rate and exhibited excellent cycling stability.

1. Introduction

Currently lithium ion batteries are being used in such portable devices as cell phones and notebook computers and in many telecommunication applications. These batteries show promise for future use as power sources in hybrid electric vehicles because of their high voltage and long cycling life. One of the key safety issues in LIBs for HEVs would be the dendritic lithium ion growth on the anode surface at high charging current, since the conventional carbonous materials approach almost 0 V vs. Li/Li^+ at the end of Li insertion [1–3]. Recently, various anode materials with improved reversible capacity and stability over commercial graphite have been proposed for Li-ion batteries. Among anode materials, $Li_4Ti_5O_{12}$ has 3-D Li^+ diffusion pathway and negligible structure change during charge–discharge cycling [4–6]. It features a flat working voltage of about 1.5 V vs. lithium, which is higher than the reduction potential of common electrolyte solvent. Although $Li_4Ti_5O_{12}$ anode material has many advantages, it cannot meet the need of practical application owing to its poor electronic conductivity [7–11]. Therefore, the electrochemical of $Li_4Ti_5O_{12}$ might not be sufficient for high current applications before any modification.

The electrochemical performance of the electrode materials depends on the synthesis method and route, leading to various particle size and morphology of the products [12,13]. To overcome the poor electronic conductivity of $Li_4Ti_5O_{12}$ anode material, many works have been concentrated on synthesis method [14–17]. However, these proposed methods have such disadvantages as they are too complicated and have only been utilized in small-scale applications, making them difficult to commercialize. Usually, conventional solid state cannot provide the required particle size and homogeneity, which affects the electrochemical properties of the products [18]. Especially, the raw materials of sol–gel method includes organic acid, which has a high synthesized cost and easily causes the aggregation of particles during calcinated process. Therefore, this study aims to provide a modified solid state method to synthesize $Li_4Ti_5O_{12}$. The method provides not only a porous morphology but also low cost and less aggregation of particle. In a previous study, the electrochemical performance of porous $LiNi_{0.5}Mn_{1.5}O_4$ cathode material was significantly improved after prolong cycling [19]. The porous structure $Li_4Ti_5O_{12}$ can efficiently reduce the diffusion pathway of lithium ions and enhance the electron transport. To our knowledge, this kind of synthetic approach and particle morphology has not been published. It is expected that the porous $Li_4Ti_5O_{12}$ structure can provide favorable electrochemical properties and rate ability at RT.

2. Experiment

Appropriate amounts of LiCl and 70 wt% oxalic acid were thoroughly mixed, and then $TiCl_4$ was rapidly introduced using a dropper. The precursor was heated at 150 °C for 0.5 h on a hot plate. Finally, it was sintered at 400 °C for 3 h and then calcined at 800 for 10 h in air to synthesize the porous $Li_4Ti_5O_{12}$.

The crystal structure of the fresh $Li_4Ti_5O_{12}$ anode material was identified by powder XRD (Rigaku, D/MAX-B, Japan) using Cu Kα radiation at 30 kV and 20 mA. Particle size and morphology of the $Li_4Ti_5O_{12}$ powder were examined with a field emission scanning electron microscope (FE-7600, JEOL). The $Li_4Ti_5O_{12}$ electrode sheets employed for electrochemical examinations were fabricated by mixing

* Corresponding author.
E-mail address: jgd@mx.nthu.edu.tw (J.-G. Duh).

0925-8388/$ – see front matter © 2010 Elsevier B.V. All rights reserved.
doi:10.1016/j.jallcom.2010.12.160

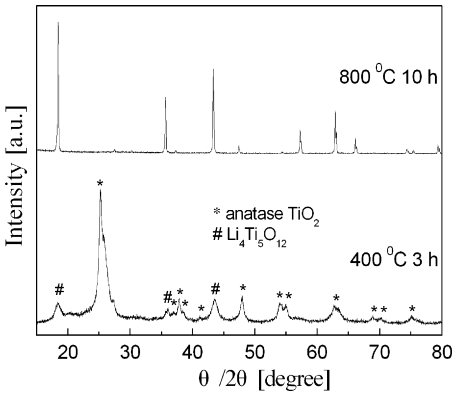

Fig. 1. X-ray diffraction pattern for $Li_4Ti_5O_{12}$ obtained at 400 and 800 °C.

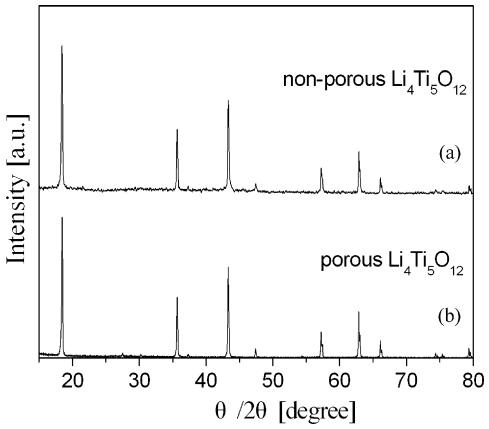

Fig. 3. XRD patterns of (a) non-porous $Li_4Ti_5O_{12}$ prepared by conventional solid state method; (b) porous $Li_4Ti_5O_{12}$ synthesized by one-step solid state method.

$Li_4Ti_5O_{12}$ powder with conductive carbon (super P) and binder (PVDF) at a weight ratio of 80:13:7 in N-methyl-2-pyrrolidinone (NMP). The anode sheet was prepared by casting the slurry in Cu foil and drying at 100 °C for 24 h in vacuum. A Li metal disk was used as an anode and reference in the cell. A 2032 coin cell was fabricated by combining the $Li_4Ti_5O_{12}$ anode and Li metal cathode in a stainless steel button cell containing electrolyte, which was 1 M $LiPF_6$ dissolved in a 1:1 mixture by volume of ethylene carbonate (EC) and dimethyl carbonate (DMC). The cells were assembled in an argon-protected glove box in which water content was kept below 0.1 ppm and all of the cells were cycled within the potential range between 2.5 and 1.0 V at different *C* rates.

3. Results and discussion

In this study, by using a modified one-step solid-state reactions method with 70 wt% oxalic acid, $Li_4Ti_5O_{12}$ powders with porous structure were synthesized. First, LiCl and 70 wt% oxalic acid, used as the starting materials, were mixed thoroughly for 0.5 h. Then $TiCl_4$ with a dropper was dripped into the beaker quickly to avoid the hydrolysis of $TiCl_4$. Mixing of $TiCl_4$ and oxalic acid resulted in the metathesis reaction and an acid mist of HCl was emitted during the process. Following the synthesis, the precursor was sintered at 400 °C for 3 h to destroy the organic framework. Oxalic acid formed a mixed precursor, acting as substrate for the homogeneous distribution of the metal oxide phase, and upon calcination in air, the carbonaceous substrate was oxidized to CO_2. Due to the release of gas, the products left behind a divided oxide phase and avoided the aggregation of particles during the synthesized process. Finally, the $Li_4Ti_5O_{12}$ powder was synthesized at 800 °C for 10 h to prepare the porous $Li_4Ti_5O_{12}$. The XRD pattern of the sample obtained at 400 °C for 3 h exhibits the characteristic diffraction lines of anatase TiO_2 and small amounts of $Li_4Ti_5O_{12}$, as shown in Fig. 1. The anatase TiO_2 can accommodate much more lithium in its crystal lattice compared to rutile TiO_2. So, once rutile TiO_2 was formed, the formation of $Li_4Ti_5O_{12}$ was suppressed due to its much worse reactivity than anatase TiO_2 [20,21]. It is thus anticipated that pure $Li_4Ti_5O_{12}$ can be synthesized by a one-step solid state method. The diffraction peaks are in good agreement with those of the JCPD powder file no. 490207, indicating that the obtained powders have a cubic spinel structure. The lattice parameter of the $Li_4Ti_5O_{12}$ obtained according to the Rietveld method was 0.8354 nm, which was consistent with the $Li_4Ti_5O_{12}$ synthesized by Li et al. [22]. The surface morphology and particle size of porous $Li_4Ti_5O_{12}$ were analyzed by FE-SEM, as shown in Fig. 2. The porous structure is helpful for increasing the contact area between the electrode and the electrolyte and thus enhancing the lithium ion diffusion process and electron transport. It is anticipated that the electrochemical properties of the powders should exhibit an excellent cycling life and rate ability.

To compare the different performances of $Li_4Ti_5O_{12}$ synthesized by conventional solid state method and one-step method developed in this study, the non-porous $Li_4Ti_5O_{12}$ was synthesized by conventional solid state method. The non-porous $Li_4Ti_5O_{12}$ was prepared from TiO_2 (<25 nm, anatase structure) and LiCl by using conventional solid state method. The starting materials, TiO_2 and LiCl in a Li:Ti molar ratio of 4:5 were mixed and ball-milled for 5 h. The powder was then calcinated 800 °C for 10 h in air. The XRD of non-porous $Li_4Ti_5O_{12}$ is shown in Fig. 3. The crystal size was 51 and 41 nm according to the Scherrer equation and the lattice parameter was 0.8354 and 0.8372 nm by the Rietveld method for porous $Li_4Ti_5O_{12}$ and non-porous $Li_4Ti_5O_{12}$, respectively. It is apparent that the primary particle size and lattice constant are almost the same in both samples. However, the morphology and electrochemical prop-

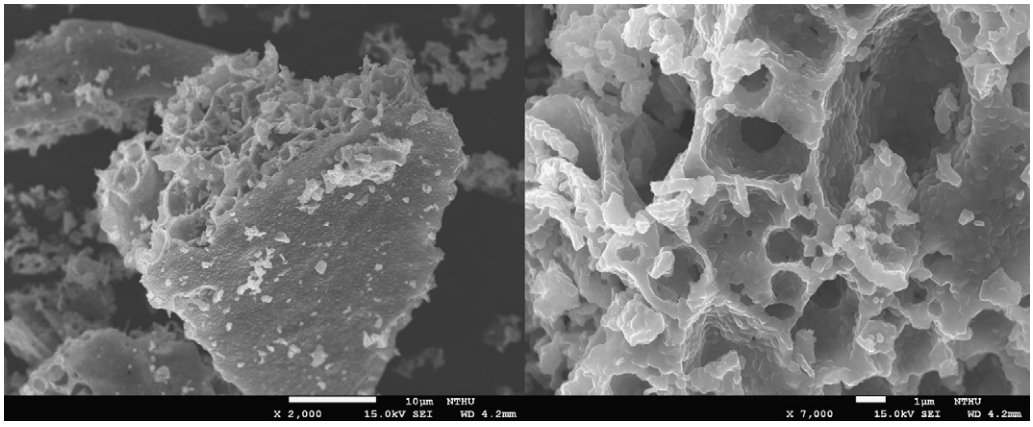

Fig. 2. FE-SEM morphology of $Li_4Ti_5O_{12}$ with porous structure.

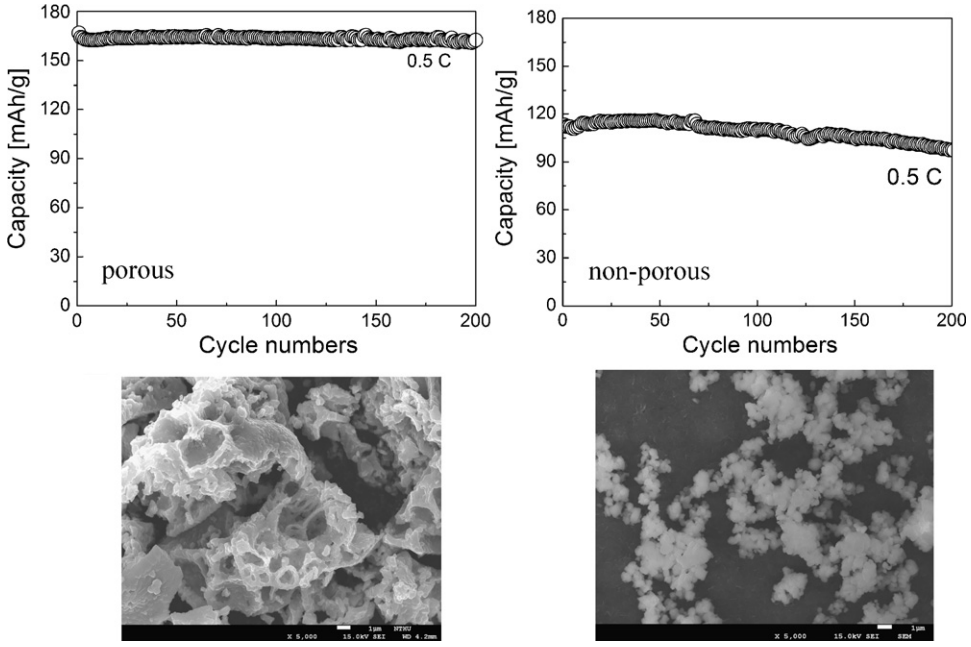

Fig. 4. The electrochemical properties of porous and dense morphology at 0.5 charge/discharge rate.

erties appear evidently different, as shown in Fig. 4. The particles of non-porous $Li_4Ti_5O_{12}$ are aggregated. In general, the aggregation is a big problem associated with sol–gel or conventional solid state method [23–27]. It causes lower capacity and poorer rate capability. The non-porous $Li_4Ti_5O_{12}$ had a capacity of 115 mAh g^{-1} at 0.5*C* (87.5 mA) charge/discharge rate (Theoretically capacity of $Li_4Ti_5O_{12}$ is 175 mAh g^{-1}). In contrast, the porous $Li_4Ti_5O_{12}$ showed a capacity of 167 mAh g^{-1} at the same charge/discharge rate. To further understand the differences of the porous and dense $Li_4Ti_5O_{12}$ on the electrochemical performance, all the samples were investigated by EIS. EIS is a versatile technique for studying the kinetics of electrochemical system. Fig. 5 shows the impedance spectra of the porous and dense $Li_4Ti_5O_{12}$ cells which were discharged to 1.5 V. Each plot consists of one semicircles at higher frequency followed by linear part at lower frequency. The low frequency region of the straight line is attributed to the Warburg impedance of long-range lithium ion diffusion. The diffusion coefficient of Li^+ for the porous and dense $Li_4Ti_5O_{12}$ is 2.86×10^{-9} and 1.10×10^{-10} cm^2/s, respectively. The porous $Li_4Ti_5O_{12}$ has better rate capability and higher capacity than dense $Li_4Ti_5O_{12}$, which is attributed to the lower cell resistance and larger diffusion coefficient of Li^+.

Fig. 6 shows the galvanostatic charge–discharge curves of porous $Li_4Ti_5O_{12}$ at 0.5*C* charge/discharge rate. The charge and discharge curves display very flat plateau at the potential of about 1.5 V, demonstrating the characteristic of two-phase reaction based on the Ti^{4+}/Ti^{3+} redox couple. The coulombic efficiency of charge and discharge is near 100% at 0.5*C* rate after 200 cycles, implying that the electrochemical reversibility of the porous $Li_4Ti_5O_{12}$ is excellent with an increase in the number of cycles. Fig. 7(a) illustrates the charge/discharge curves of porous $Li_4Ti_5O_{12}$ at a charge/discharge rate of 0.5 and 1*C* (175 mA). The porous $Li_4Ti_5O_{12}$ delivers 167 mAh g^{-1} at 0.5*C* charge/discharge rate, which is very close to the theoretical capacity 175 mAh g^{-1}, while it exhibits 133 mAh g^{-1} at a higher charge/discharge rate (1*C*). The capacity retention is as high as 98% and the average discharge capacity loss per cycle is rather low at 0.01 loss/cycle over 200 cycles. Fig. 7(b) depicts the rate capability of the porous $Li_4Ti_5O_{12}$ charged at 0.5*C* and discharged at different *C* rate. It is evident that the porous $Li_4Ti_5O_{12}$ without any doping or coating carbon could exhibit good cycling stability from 0.5 to 30*C* discharge rate. The porous $Li_4Ti_5O_{12}$ shows a capacity of 150 mAh g^{-1} at 1*C* discharge rate, and even reaches ~80 $mAhg^{-1}$ at a much higher discharge rate of 10*C*. An appropriate electrode material must meet the requirements for battery operation under practical conditions, and it should be

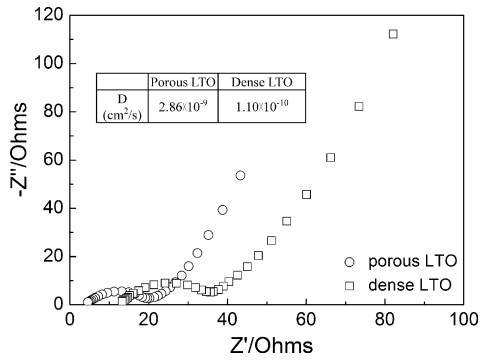

Fig. 5. AC impedance spectra of the dense and porous $Li_4Ti_5O_{12}$ cell.

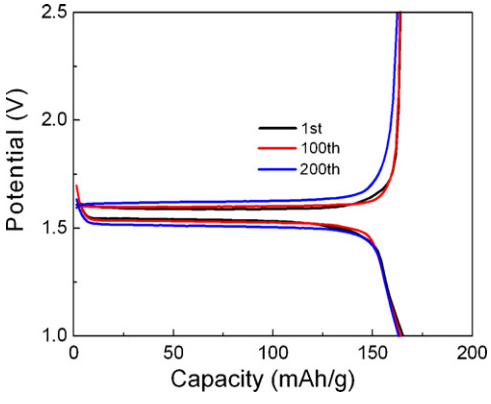

Fig. 6. Galvanostatic charge–discharge curves of porous $Li_4Ti_5O_{12}$ at 0.5*C* charge/discharge rate.

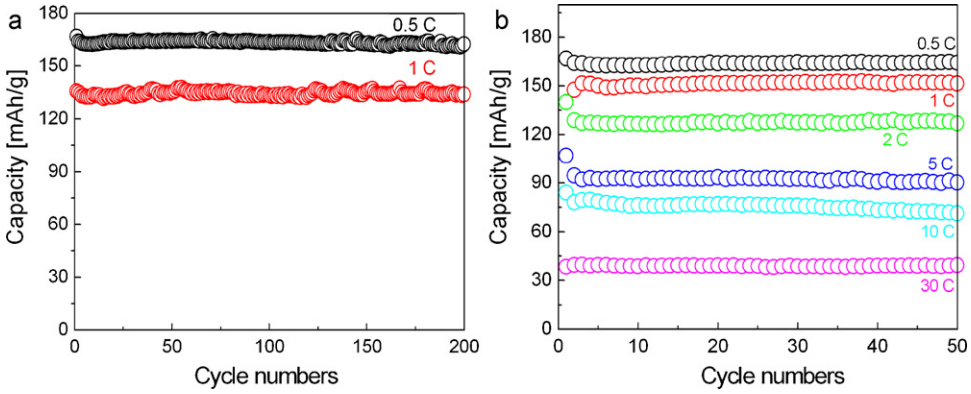

Fig. 7. (a) Electrochemical performance of $Li_4Ti_5O_{12}$ with porous structure at charged/discharge 0.5 and 1*C* rate; (b) rate performance at charged at 0.5*C* and discharged at different *C* rate.

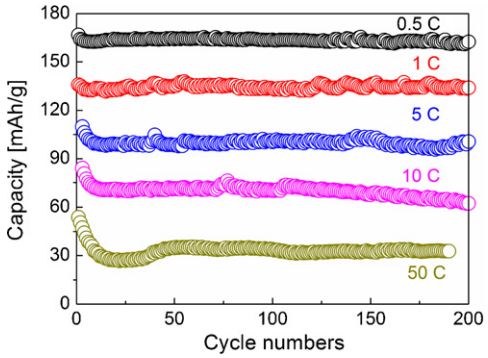

Fig. 8. Electrochemical performance of porous $Li_4Ti_5O_{12}$ at different charge/discharge rate. By using a simple one-step solid-state reactions method synthesizes a porous $Li_4Ti_5O_{12}$.

able to withstand the rapid charging/discharging. Fig. 8 shows the fast charge/discharge rate of porous $Li_4Ti_5O_{12}$. The capacity of porous $Li_4Ti_5O_{12}$ showed 167, 133, 100, 70, 30 mAh g^{-1} at 0.5, 1, 5, 10 and even 50*C* charge/discharge rate, respectively, and the capacity retention exhibited excellent cycling stability after 200 cycles.

On the basis of above results, the porous $Li_4Ti_5O_{12}$ prepared by one-step solid state method is beneficial for reducing the pathway of lithium ion and electron transport, which can enhance the electrochemical properties and rate ability for prolong cycling.

4. Conclusion

Mixtures of LiCl and $TiCl_4$ with 70 wt% oxalic acid were employed by one-step solid-state reactions method to successfully synthesize porous $Li_4Ti_5O_{12}$ anode material, exhibiting outstanding electrochemical properties. The initial capacity was 167 and 133 mAh g^{-1} at 0.5 and 1*C* charge/discharge rate, respectively and capacity retention maintained at 98% at RT after 200 charge/discharge cycles. At a much higher charge/discharge rate such as 10 and 50*C*, the porous $Li_4Ti_5O_{12}$ anode material without doping any element or coating carbon could reach ~70 and 30 mAh g^{-1}, respectively after 200 cycles.

Acknowledgements

This study was financially supported by National Science Council of Taiwan, under project no. NSC 96-2221-E-007-093-MY3 and from the Ministry of Economics under the project No. 98-EC-17-A-08-S1-003.

References

[1] T.F. Yi, L.J. Jiang, J. Shu, C.B. Yue, R.S. Zhu, H.B. Qiao, J. Phys. Chem. Solids 71 (2010) 1236.
[2] T. Ohzuku, A. Ueda, N. Yamamoto, J. Electrochem. Soc. 142 (1995) 1431.
[3] C.Y. Ouyang, Z.Y. Zhong, M.S. Lei, Electrochem. Commun. 9 (2007) 1107.
[4] M. Venkateswarlu, C.H. Chen, J.S. Do, C.W. Lin, T.C. Chou, B. Hwang, J. Power Sources 146 (2005) 204.
[5] J.L. Allen, T.R. Jow, J. Wolfenstine, J. Power Sources 159 (2006) 1340.
[6] J.J. Huang, Z.Y. Jiang, Electrochim. Acta 53 (2008) 7756.
[7] Z. Lin, X. Hu, Y. Huai, L. Liu, Z. Deng, J. Suo, Solid State Ionics 181 (2010) 412.
[8] P.P. Prosini, R. Mancini, L. Petrucci, V. Contini, P. Villano, Solid State Ionics 144 (2001) 185.
[9] Y.J. Hao, Q.Y. Lai, D.Q. Liu, Z. Xu, X.Y. Ji, Mater. Chem. Phys. 94 (2005) 382.
[10] A. Guerfi, P. Charest, K. Kinoshita, M. Perrier, K. Zaghib, J. Power Sources 126 (2004) 163.
[11] P.G. Bruce, B. Scrosati, J.M. Tarascon, Angew. Chem. Int. Ed. 47 (2008) 2930.
[12] S.Y. Yin, L. Song, X.Y. Wang, M.F. Zhang, K.L. Zhang, Y.X. Zhang, Electrochim. Acta 54 (2009) 5629.
[13] Y.F. Tang, L. Yang, Z. Qiu, J.S. Huang, Electrochem. Commun. 10 (2008) 1513.
[14] J.R. Li, Z.L. Tang, Z.T. Zhang, Electrochem. Commun. 7 (2005) 894.
[15] D. Takayuki, I. Yastutoshi, A. Takeshi, O. Zempachi, Chem. Mater. 17 (2005) 1580.
[16] H. Liu, Y. Feng, K. Wang, J.Y. Xie, J. Phys. Chem. Solids 69 (2008) 2037.
[17] A.J. Patil, M.H. Shinde, H.S. Potdar, Mater. Chem. Phys. 68 (2001) 7.
[18] K. Zaghib, M. Simoneau, M. Armand, M. Gauthier, J. Power Sources 81–82 (1999) 300.
[19] C.Y. Lin, J.G. Duh, C.H. Hsu, J.M. Chen, Mater. Lett. 64 (2010) 2328.
[20] T. Yuan, R. Cai, P. Gu, Z. Shao, J. Power Sources 195 (2010) 2883.
[21] T. Yuan, X. Yu, R. Cai, Y. Zhou, Z. Shao, J. Power Sources 195 (2010) 4997.
[22] X. Li, M. Qu, Z. Yu, J. Alloys Compd. 487 (2009) L12.
[23] S. Bach, J.P. Pereira-Ramos, N. Baffier, J. Power Sources 81–82 (1999) 273.
[24] S. Batch, J.P. Pereira-Ramos, N. Baffier, J. Mater. Chem. 8 (1998) 251.
[25] M. Venkateswarlu, C.H. Chen, J.S. Do, C.W. Lin, T.C. Chou, B.J. Hwang, J. Power Sources 146 (2005) 204.
[26] K.C. Hsiao, S.C. Liao, J.M. Chen, Electrochim. Acta 53 (2008) 7242.
[27] C.H. Jiang, Y. Zhou, I. Honma, T. Kudo, H.S. Zhou, Electrochim. Acta 166 (2007) 514.